



http://pubs.acs.org/journal/acsodf Article

Probing the Dynamics of AcrB Through Disulfide Bond Formation

Prasangi Rajapaksha, Ankit Pandeya, and Yinan Wei*



Cite This: ACS Omega 2020, 5, 21844-21852



ACCESS

Metrics & More

Article Recommendations

ABSTRACT: The resistant-nodulation-division (RND) superfamily member tripartite AcrA-AcrB-TolC efflux pump is a major contributor to the multidrug resistance in *Escherichia coli*. AcrB is the inner membrane protein of the efflux complex and is responsible for the recognition and binding of compounds before their transportation out of the cell. Understanding the dynamics of AcrB during functional rotation in the process of drug efflux is the focus of this study. For this purpose, we introduced six inter-subunit disulfide bonds into the periplasmic domain of AcrB using site-directed mutagenesis to



study the importance of the relative flexibility at the inter-subunit interface. Western blot analysis revealed the formation of disulfide bond-linked AcrB oligomers, which were reduced into monomers under reducing conditions. The impact of mutation and formation of disulfide bond on efflux were evaluated via comparison of the minimum inhibitory concentration (MIC) of an *acrB* knockout strain expressing different mutants. The double Cys mutants tested led to equal or higher susceptibility to AcrB substrates compared to their corresponding single mutants. To determine if the reduction of activity in a double mutant is due to restriction on conformational changes by the disulfide bond formation, ethidium bromide accumulation assays were conducted utilizing dithiothreitol (DTT) as the reducing agent. In two cases, the activities of the double Cys mutants were partially restored by DTT reduction, confirming the importance of relative movement in the respective location for function. These findings provide new insights into the dynamics of the AcrAB-TolC efflux pump in *E. coli*.

1. INTRODUCTION

The multidrug resistance in bacteria has become one of the major threats in global health. Bacteria have developed a mechanism to evade the attack of most commercially available drugs. In gram-negative bacteria such as Escherichia coli, multidrug efflux systems are a major mechanism that confers intrinsic and increased drug resistance to a broad spectrum of antimicrobials.1 The overexpression of resistant-nodulationdivision (RND) superfamily member AcrAB-TolC, a tripartite complex that spans through the outer membrane and the inner membrane, has been identified as an important mechanism leading to multidrug resistance. 2-4 AcrAB-TolC is one of the major efflux systems contributing to the multidrug resistance in E. coli. This pump has an important role in transporting substances such as antibiotics, detergents, dyes, and free fatty acids out of the cell. 5-8 In this protein complex, TolC is a homotrimeric outer membrane channel that enables the exit of drugs from the cell to the external medium. AcrA belongs to the membrane fusion protein (MFP) family and exists in the periplasm. AcrB is a homotrimer inner membrane antiporter that couples the inward proton transport with the outward substrate transport. The assembly of the AcrAB-TolC tripartite complex has a stoichiometry of 3:6:3 for TolC:AcrA:AcrB, respectively.6,9

The assembled structure of the AcrAB-TolC pump complex has been revealed in several scanning electron microscopy studies, ^{6,10} and more recently through cryoEM studies, which provides insight into the molecular mechanism of transport by

this pump. ^{11,12} Moreover, symmetric and asymmetric crystal structures of AcrB in the apo and substrate-bound states has been determined. ^{13–19} The antiporter AcrB functions as a trimer, with 12 transmembrane α helices and a large periplasmic domain in each subunit. ¹¹ AcrB plays a pivotal role in the recognition and binding of substrates and harvests the proton motive force to energize drug efflux. In the periplasmic domain of each subunit, there are multisite drugbinding pockets, which enable a broad range of drugs to enter and bind, and subsequently exit through efflux. ^{20,21}

The asymmetric structure of AcrB revealed novel insight into the drug binding and transport mechanism of the pump. The AcrB periplasmic domain divides into two domains, the porter (pore) domain and the funnel (previously known as "docking") domain (Figure 1). Porter domain is further categorized into four subdomains as PN1, PN2, PC1, and PC2. The funnel domain has two major subdomains, DC and DN. PN1 and PC2 subdomains together form a rigid β - sheet structure, in a similar way PN2 and PC1 form a β -sheet. Hence, in previous reports, the porter domain has been divided into two structural subunits called PN1–PC2 and PN2–

Received: June 17, 2020 Accepted: August 5, 2020 Published: August 20, 2020





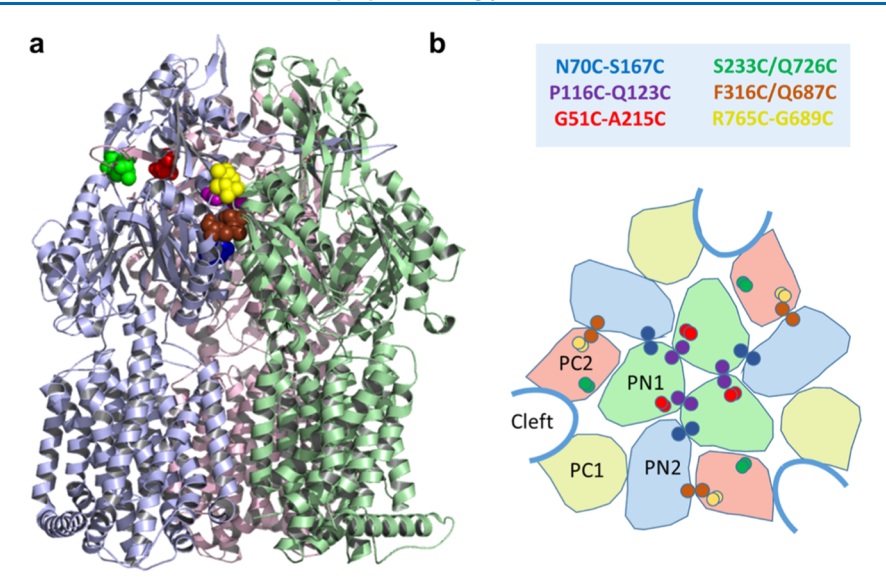


Figure 1. Locations of the six Cys pairs in the structure of AcrB. (a) Structure of an AcrB trimer showing the color-coded Cys pairs. Only mutated residues in the light purple subunit and their partners are shown for clarity. (b) Organization of the subdomains in the porter domain. The locations of disulfide bonds are shown as dots. Structure image is rendered with pymol (https://pymol.org/2/) using the asymmetric structure 2HRT.pdb. 26

PC1. ^{22,23} The substrate access and transport pathway is formed between these two structural units. The analysis of crystal structures has revealed that a distal/deep binding pocket is located in the PN2–PC1 unit. Subdomains PC1 and PC2 form the cleft in the bottom of the periplasmic domain, which is another drug-binding pocket termed the proximal binding site. PN1 and PN2 form the drug exit pathway connecting to the central pore. ^{15,23,24}

Substrates can access the AcrB binding pocket from the periplasm or the outer leaflet of the inner membrane, through entry points/vestibules near promoters. ¹⁵ More recently, some studies suggest that certain substrates could gain access from the cytoplasm through the central cavity or the transmembrane-embedded external surface of the trimer.^{8,25} In the asymmetric AcrB structure, each protomer exhibits conformational differences representing each stage of the drug transport cycle, open access (loose—L), drug binding (tight—T), and drug extrusion (open—O). 15,26,27 This proposed mechanism is termed the peristaltic functional rotation mechanism. 15,26-31 According to the functional rotation mechanism, the external cleft between the PC1 and PC2 subdomains opens and closes, thus changes the distances between the protomers at the periplasmic domain. In the binding conformation, the cleft opens wide. Also, in the extrusion conformation, the cleft closes through the movement of the PC1 and PC2 subdomains. These conformational changes are due to proton translocation across the transmembrane domain and drug binding to the porter domain.

Disulfide bond trapping is an effective method in studying the conformational changes in proteins. Cysteine residues are introduced into the desired locations through site-directed mutagenesis, and then disulfide bond formation is monitored. For proteins in gram-negative bacteria, sites located in the periplasmic domain are normally chosen for mutation since disulfide bonds form readily in this cellular compartment.³² In this study, we introduced inter-subunit disulfide bonds in the periplasmic domain of AcrB. Through ethidium bromide (EtBr) accumulation assays and drug susceptibility assays, we have investigated how the Cys mutation and disulfide bond

introduced at each specific location affected the function of AcrB.

2. RESULTS AND DISCUSSION

2.1. Inter-Subunit Disulfide Cross-Linking Construction. The functional rotation mechanism proposed first in 2006 highlighted the importance of AcrB conformational change during substrate efflux. 15,26 During this three-step mechanism, each protomer of the AcrB trimer adopts a distinct conformation. The conformational changes are driven by the proton translocation into the cytoplasm from the periplasm through a pathway along the transmembrane domains of AcrB. As discussed above, the relative locations of the periplasmic subdomains change during the functional rotation. This cycling mechanism suggested that AcrB acts as a peristaltic pump through the opening and closing of the drug-binding pockets and access to the TolC. Furthermore, it has been speculated that the conformational changes caused by substrate binding and proton motive force may transfer through AcrA bound to the cleft. 15 Using the online server of "Disulfide by Design 2.0" (http://cptweb.cpt.wayne.edu/DbD2/),³³ we identified six sites on the inter-subunit interface to introduce Cys pairs and used these pairs to study the flexibility and relative conformational change at the corresponding locations.

The locations of the six cys pairs are shown in Figure 1. Residues G51, N70, Q123, and P116 are located in the PN1 subdomain. S167 and F316 are in the PN2 subdomain. Q687 and G689 are in the PC2 domain. A215 and S233 exist in the long-extended loop that penetrates deep into the neighboring subunit. R765 exists at the tip of a long loop formed by the Cterminal half of AcrB, which is equivalent to the extended loop in the N-terminal half of AcrB. Q726 is located at the boundary between PC2 and the DC domain. These introduced cysteine pairs were expected to form crosslinks at the intersubunit interface between the PN1-PN2 subdomains (N70C/ S167C), PN1-PN1 subdomains (P116C/Q123C), PN2-PC2 subdomains (F316C/Q687C), the loop and DC subdomain (S233C/Q726C), the loop and PN1 subdomain (G51C/ A215C), and the PC2-DC subdomains (G689C/R765C). From the four subdomains in the porter domain, PN1-PC2

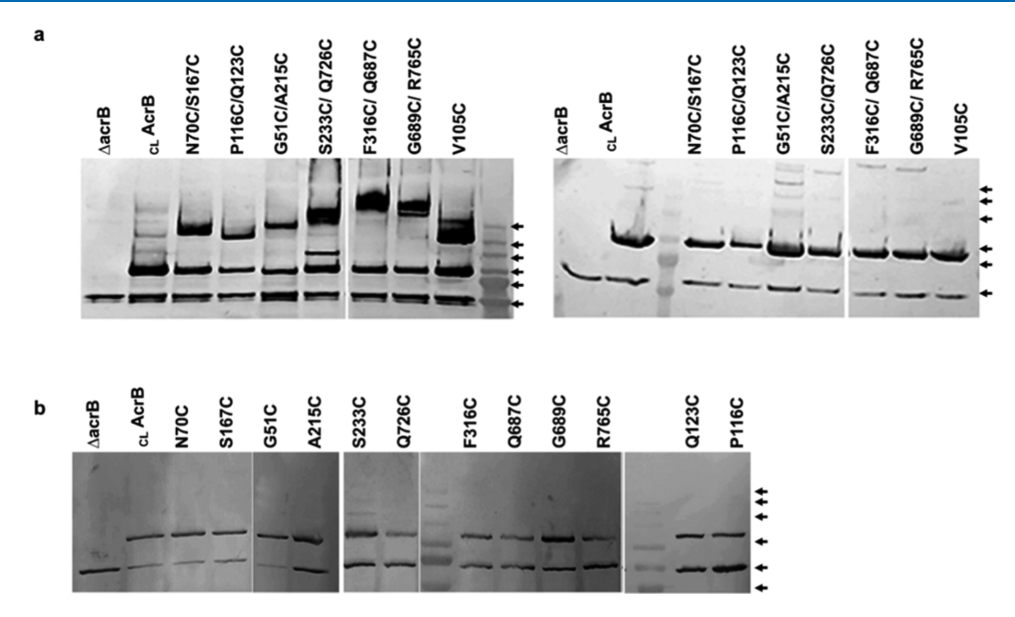


Figure 2. Western blot analysis of disulfide bond formation in AcrB mutants. (a) Double-cysteine mutants, with nonreduced samples shown on the left and reduced samples shown on the right. (b) Single-cysteine mutant samples without reduction. Bands in the molecular weight marker are highlighted using black arrows. From top to bottom, the arrows correlate with molecular weights of 245, 190, 135, 100, 80, and 58 kDa.

Table 1. Percentage of Oligomers in Mutants

AcrB mutants	N70C/S167C	P116C/Q123C	G51C/A215C	S233C/Q726C	F316C/Q687C	G689C/R765C	V105C
oligomer (%)	58.3 ± 5.4	53.2 ± 11.4	60.6 ± 6.8	69.1 ± 6.6	68.9 ± 6.4	74.9 ± 6.8	57.9 ± 13.2

and PN2–PC1 form the binding pockets. The proximal binding site involves PC1–PC2 interaction, and PN1–PN2 is important in the exit stage of the substrate. Furthermore, V105C in the PN1 domain, which has been reported to form a disulfide bond in an AcrB trimer, was used as a control to reveal the migration position of a disulfide bond-linked dimer. Cell lysate samples prepared from BW25113 $\Delta acrB$ and BW25113 $\Delta acrB$ transformed with plasmid pQE70-CLAcrB were used as the controls. In CLAcrB, two intrinsic Cys residues were replaced with Ala.

2.2. Detection and Quantification of Disulfide Bond Formation. The formation of disulfide crosslinks was analyzed using Western blot analysis with an anti-AcrB antibody. In the absence of the reducing reagent, all six pairs formed oligomers (Figure 2a). IAM was added before the lysis of the cells to prevent the formation of a disulfide bond during the cell lysis and analysis process. An unknown band close to the 58 kDa marker could be observed in all samples, including the negative control. This band has been observed in previous studies using the same antibody.³⁵ It could be an unknown protein that also contains a stretch of a similar peptide like the one used to raise the antibody. Since this nonspecific band is well separated from those of the AcrB band, it does not interfere with the interpretation of the data. The intensity of this nonspecific band also served as a loading control. Otherwise, the cell lysate prepared from BW25113 $\Delta acrB$ did not have a protein band, confirming the good specificity of the antibody. The background construct CLAcrB migrated with an apparent molecular weight of ~100 kDa, consistent with a monomer. The oligomers formed by other Cys pair constructs are likely dimer or trimers. The treatment with 10% β mercaptoethanol led to a complete reduction of oligomers to monomers, further confirming that the high-molecular-weight bands were formed due to disulfide bonds. The expression

level of most Cys pair constructs was similar to that of CIAcrB, while the P116C/Q123C pair seemed to express significantly less. Furthermore, Western blot analysis of single-cysteine mutations revealed that no high-molecular-weight oligomers were present, confirming that disulfide bonds were formed between the pair of cysteines (Figure 2b). The mobility of oligomers was different for different Cys pairs. In an AcrB trimer containing a Cys pair at each inter-subunit interface, there are four possible products: a circular trimer trapped with three disulfide bonds, a linear trimer trapped with two disulfide bonds, and a disulfide bond trapped dimer plus a monomer. We included V105C in this study as a mobility marker, as it would migrate as a monomer and a disulfide bond-linked dimer. Through comparison with the V105C dimer bands, it appeared that the mobility of P116C/Q123C, G51C/A215C, and N70C/S167C oligomers seemed to be closer to that of the V105C dimer with an apparent molecular weight of ~200 kDa, and the oligomer formed in F316C/Q687C, G689C/R765C, and S233C/Q726C constructs migrated slower than the V105C dimer and with apparent molecular weight larger than the highest band in the marker (245 kDa). Disulfide bond introduced at different locations has a clear impact on the mobility of the protein.

While all Cys pair mutants formed a significant portion of disulfide bond-linked oligomers, they all have a monomer population. We used the software ImageJ to analyze the percentage of crosslinked products in each of the mutants.³⁶ The percentage of crosslinked oligomers ranged from 53 to 75% (Table 1). Several factors may affect the level of disulfide bond formation between two residues in the structure of a protein, the distance between the residues, the compatibility of the geometry of the Cys pair to that of a disulfide bond, and the intrinsic flexibility of the relevant protein regions including both the backbone and the side chain (the B-factor).³³ We

noted that one of the Cys pairs we created in this study, S233C/Q726C, have been reported in a previous study by Seeger et al. The previously reported cross-linking level of $17.0 \pm 0.4\%$ is significantly lower than our observation (69.1 \pm 6.6). The difference could be due to differences in the cell culture and sample procession procedure. An extra band could be observed at ~120 kDa, which disappeared upon reduction. We speculate that this could be a different protein conformation that was trapped by the disulfide bond. This band could also be observed, although at a lower concentration, in the study by Seeger et al. The provious study of the disulfide bond.

2.3. Functional Analysis of Cysteine Mutations through Drug Susceptibility Assay. To evaluate the impact of the introduced Cys mutations and subsequent formation of disulfide bond on AcrB function, we measured the MIC of BW25113 $\Delta acrB$ transformed with plasmids encoding each single or double Cys mutant. Four known AcrB substrates were used in the assay (Table 2). If relative movement at the respective sites is important for efflux, we expect the formation of disulfide bonds at these sites would affect protein function.

Table 2. MIC (μg/mL) Values for E. coli BW25113ΔacrB Containing Single- or Double-Cysteine AcrB Mutants

plasmid	novobiocin	erythromycin	EtBr	TPP
none	8	4	16	16
$_{\mathrm{CL}}\mathrm{AcrB}$	128	128	256	512
S167C	64	64	128	512
N70C	128	64	128	512
N70C/S167C	64	64	128	512
Q123C	64	64	128	256
P116C	64	64	256	512
P116C/Q123C	32	64	128	256
G51C	64	128	128	256
A215C	128	128	256	512
G51/A215C	64	128	128	256
Q726C	64	128	256	512
S233C	128	128	256	512
S233C/Q726C	64	128	256	512
F316C	64	64	256	512
Q687C	128	128	256	512
F316C/Q687C	16	16	32	32
R765C	64	64	256	512
G689C	64	64	256	512
G689C/R765C	32	32	128	256
V105C	16	32	64	128
V105G	32	32	128	128

The behavior of the constructs could be clustered into two groups. In the first group, the Cys pair mutants behaved similarly as the less active single mutant for most of the substrates tested. Four out of the six constructs belonged to this group. Strains containing N70C, S167C, or the N70C/S167C double mutant all had similar MIC values as the positive control CLACTB for TPP, while the MIC of the other three compounds was reduced by half. The Q123C mutation reduced the MIC of all four drugs tested by half, while the P116C mutation only affected the MIC of novobiocin and erythromycin. The double mutant P116C/Q123C behaved similar to the single Q123C mutant except for novobiocin, for which the MIC was further reduced by 2-fold. The G51C single mutation led to a 2-fold reduction of the MIC of

novobiocin, EtBr, and TPP, while the A215C mutation did not lead to an MIC change. Strains containing the G51C/A215C double mutation had similar MIC as the G51C single mutant for all four test compounds. Strains containing Q726C, S233C, or the corresponding double mutant had similar MIC as the positive control for all substrates except for novobiocin. The Q726C single mutant and the double mutant displayed a 2-fold reduction in MIC for novobiocin.

The other two pairs belong to the second group. For the F316C/Q687C pair and the G689C/R765C pair, strains containing the double mutants displayed lower MICs for all four compounds tested than the corresponding single mutants. While the Q687C mutation did not lead to an observable reduction of activity, the F316C mutation led to a 2-fold reduction of MICs for novobiocin and erythromycin. The F316C/Q687C double mutant displayed an 8- to 16-fold reduction in MIC for all substrates. Similarly, R765C and G689C single mutants had similar activity as the positive control for EtBr and TPP, and a 2-fold reduction of MIC for erythromycin and novobiocin. The double mutant showed lower activity toward all four compounds with a reduction in MIC of 2- to 4-fold. For this group, there is a possibility that the observed higher susceptibility of the cysteine double mutants is due to the restriction of conformational change resulted from crosslinks, which impaired the efflux activity of AcrB. We have also included V105C and V105G mutants in this study. As expected, mutation of V105 led to a significant reduction of efflux activity as the MICs of all four compounds tested were reduced. For novobiocin and EtBr, the MICs of the strain containing V105C were 2-fold lower than that of the V105G.

2.4. Restoration of the Activity by Dithiothreitol (DTT) Detected Using EtBr Accumulation Assay. If the previously observed higher drug sensitivity is a result of disulfide bond formation, the reduction of the disulfide bonds should restore the efflux activity. This was investigated using the EtBr accumulation assay. We found that DTT at 10 mM could not fully reduce the disulfide bonds formed in our AcrB constructs, even with 4 h incubation (Figure 3). While the portion of monomers did increase after the treatment, clear oligomer bands could still be observed in all cases. And for some samples, multiple oligomer bands could be observed after this treatment, which are likely partially reduced oligomers. When incubated with 50 mM DTT, disulfide bonds could be completely reduced after 1 h incubation (Figure 3). Thus, this higher DTT concentration was used for the accumulation assay. Cells containing the indicated plasmids were prepared as described in Section 4 for the EtBr accumulation assay. We included all six pairs, as well as V105C, in the study for comparison.

For four out of the six Cys pair constructs, the DTT treatment did not lead to a significant difference in the rate of EtBr accumulation (Figure 4). However, for the other two pairs, F316C/Q687C and G689C/R765C, reduced samples exhibited notably lower accumulation of EtBr, indicating that the formation of a disulfide bond contributed significantly to the reduced activity. This indicated that the reduction of disulfide crosslinks by DTT at these two locations had partially restored the efflux activity (Figure 4d,e). In a previous study by Takatsuka and Nikaido, the introduction of the F316C/Q687C double mutant has also been shown to greatly reduce the efflux activity, consistent with our observation. 27

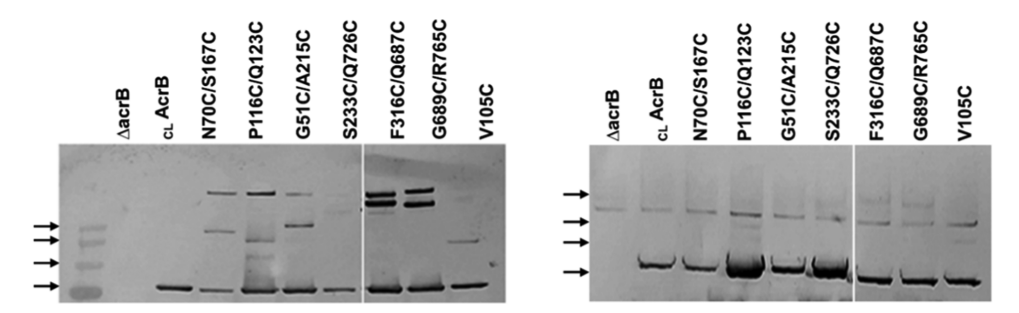


Figure 3. Anti-AcrB Western blot analysis of double-cysteine AcrB mutants under different reduction conditions. Left: Reduced with 10 mM DTT and incubated for 4 h at room temperature. Oligomers are only partially reduced. Right: Reduced with 50 mM DTT and incubated for 1 h at room temperature. Oligomers are fully reduced. The bands in the molecular weight marker are highlighted by black arrows. From top to bottom, the molecular weights are 245, 190, 135, and 100 kDa.

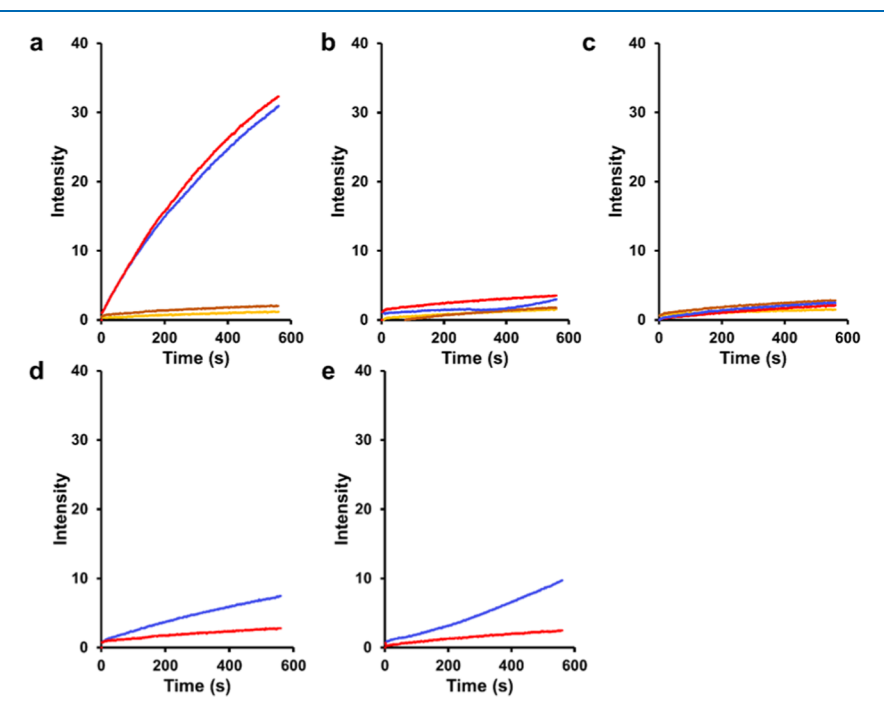


Figure 4. EtBr accumulation assay of all double-cysteine mutants with or without reduction. (a) Negative control BW25113Δ*acrB* (blue no DTT, red with DTT) and positive control BW25113Δ*acrB* expressing plasmid-coded _{CL}AcrB (orange no DTT, brown with DTT). (b) BW25113Δ*acrB* expressing AcrB mutants N70C/S167C (blue no DTT, red with DTT) or P116C/Q123C (orange no DTT, brown with DTT). (c) BW25113Δ*acrB* expressing AcrB mutants G51C/A215C (blue no DTT, red with DTT) or S233C/Q726C (orange no DTT, brown with DTT). (d) BW25113Δ*acrB* expressing AcrB mutant F316C/Q687C (blue no DTT, red with DTT). (e) BW25113Δ*acrB* expressing AcrB mutant G689C/R765C (blue no DTT, red with DTT).

2.5. V105 Mutations and Efflux. V105C is located in a helix close to the threefold axis of the AcrB trimer and forms a disulfide bond.³⁴ It was speculated that the formation of a disulfide bond restricted the conformational changes to reduce the efflux activity. In our study, we observed low MIC values (Table 2) for novobiocin and erythromycin, consistent with previous studies, indicating that the mutation significantly impacted AcrB activity.³⁴ However, the DTT treatment reduced the dimer but only led to a modest reduction of EtBr accumulation in BW25113ΔacrB expressing V105C (Figure 5). To further investigate the potential role of the disulfide bond in activity, V105 was mutated to Gly. Accumulation of EtBr in BW25113ΔacrB containing V105G was higher than that in the positive control, indicating that the replacement of Val itself is detrimental to function. This result is consistent with the MIC measurement. Accumulation of the strain containing V105C was higher than that in the strain containing V105G, suggesting that the formation of the

disulfide bond further impaired efflux. Upon reduction, accumulation in the V105C strain was reduced to be more similar to the accumulation in the V105G strain.

3. CONCLUSIONS

The structure of the entire AcrABZ-TolC complex has been revealed using cryoEM. ^{11,38} More recent studies illustrated the in situ structure of the complex in *E. coli* cells overexpressing the pump components. ¹² While these structure insights have led to the answer of many questions related to the mechanism of efflux by the RND pumps, studies on the dynamic aspects of the pumps lag far behind. As any molecular machines, the AcrAB-TolC system undergoes a conformational change to carry out efflux. While the combination of structures, which are snapshots of proteins, and computational simulation cast lights on how proteins move, experimental testing of the simulation movies is critical. Based on the crystal structure of AcrB, we

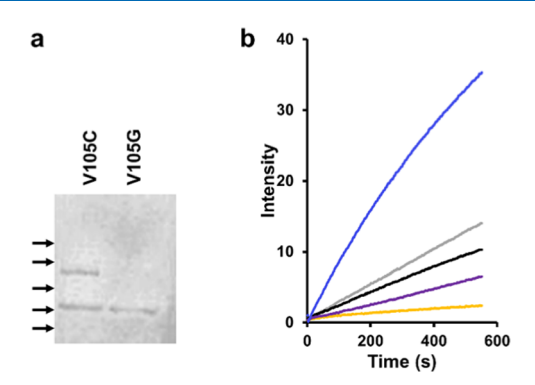


Figure 5. Analysis of V105C and V105G. (a) Anti-AcrB Western blot analysis of V105C and V105G, showing the formation of a disulfide bond in V105C but not V105G. The molecular weight of bands in the marker is highlighted by black arrows. From top to bottom: 245, 190, 135, 100, and 80 kD. (b) EtBr accumulation assay of $BW25113\Delta$ acrB expressing V105C (gray no DTT, black treated with DTT) or V105G (purple). The positive and negative controls are also shown for comparison, $BW25113\Delta$ acrB (blue) and $BW25113\Delta$ acrB expressing plasmid-coded $_{CL}$ AcrB (orange).

designed and engineered six Cys pairs to examine the consequence of these structure staples on its efflux activity. We found that for four pairs, the formation of a disulfide bond did not seem to have much impact on efflux, as the double mutant behaved similarly as the less active single mutants. Relative inter-subunit movement at these sites does not seem to be required for efflux.

For the other two pairs, the double mutants are less active than the individual single mutants, which could be potentially due to the restriction effect from the disulfide bond that either restricted relative movement of neighboring subunits or locked the subunits in a conformation incompatible with substrate binding and/or translocation. While the activity of the efflux pump is most conveniently evaluated using the MIC assay, the effect of disulfide bond on activity could not be measured this way since the high concentration of reducing reagent that is necessary to effectively reduce the disulfide bonds would inhibit E. coli growth. Alternatively, EtBr efflux could be monitored using cells containing reduced or nonreduced AcrB Cys pair constructs. We found that for two pairs, F316C/ Q687C and G689C/R765C, reduction of the disulfide bond significantly improved efflux, confirming the functional relevance of conformational flexibility at these sites. There appears to be a discrepancy between the apparent percentage of cross-linking with the level of reduced activities in these double mutants, which is most likely explained by the different growth phases the cells were harvested for the two types of experiments. For the activity (MIC) measurement, the proliferation of cells was monitored in the presence of test compounds. For the EtBr accumulation assay, mid-log phase cells were taken and used in the study, whereas for the crosslinking analysis, overnight cultures were taken, and those cells were in the stationary phase and took longer time for disulfide

Apart from the interference by disulfide bond formation on the function of AcrB, the reduction of the activity of the Cys pairs could be due to an unfavorable conformation of the disulfide dimers that interfere with the substrate binding and transport activity. Interestingly, the two sites with high impact on activity are located close to each other, with one containing Q687C and the other containing G689C, just two residues

apart (Figure 1, brown and yellow dots). While F316C/Q687C forms a disulfide bond at the interface between the PN2 and PC2 subdomain of the neighboring subunit (brown), G689C/R765C linked the PC2 subdomain to the tip of the long loop formed by the C-terminal half of the neighboring subunit.

Since each subunit in an AcrB trimer contains a separate and complete set of substrate binding residues and translocation pathway, a conformational change that is involved in substrate binding and extrusion should be localized more to the inside of a subunit. Yet, relative inter-subunit conformational change has been reported in several cases to be critical for AcrB function. likely due to the functional rotation mechanism in which the trimer needs to undergo conformational change simultaneously. Thus, some of the sites that are located at the intersubunit interface are expected to be the "sensor" sites that need to play the role of coordinating the movement. While in other sites, including several sites described in this, and V225C/ A777C, R558C/E839C, V32C/A299C, and I235C/K728C reported in previous studies (Table 3), Cys substitution and disulfide bond formation do not have a clear impact on functions.³⁷ These could be sites that maintain close contact throughout the functional rotation mechanism to maintain AcrB as a tightly associated, integrated, functional trimer.

4. EXPERIMENTAL SECTION

4.1. Bacterial Strains, Plasmids, and Growth Conditions. Plasmid pQE70- $_{\rm CL}$ AcrB, which encodes a cysless AcrB, was used as the template to create AcrB double cys mutations. The two intrinsic cysteines in $_{\rm CL}$ AcrB were both replaced by alanine to reduce the potential of nonspecific disulfide bond formation. The cysless AcrB is fully functional. Mutations were introduced using the Quikchange site-directed mutagenesis kit following the manufacturer's instruction (Agilent, Santa Clara, CA). Primers used in the study were listed in Table 4. *E. coli* strain BW25113 and BW25113 Δ acrB were obtained from Yale *E. coli* genetic resources. Bacteria were cultured at 37 °C with shaking at 250 rpm in Luria broth (LB) media unless otherwise noted.

4.2. Drug Susceptibility Assay. The MIC was determined for erythromycin, novobiocin, ethidium bromide (EtBr), and tetrapheynlphosphonium chloride (TPP) following the CLSI guidelines. ⁴² Briefly, overnight cultures of the indicated strain were diluted to a final concentration of 10⁵ CFU/mL in fresh Muller Hinton Broth 2 (cation adjusted) media (Millipore Sigma, St. Louis, MO) in a 48-well microtiter plate containing the indicated compounds at twofold serial dilutions. Plates were incubated at 37 °C with shaking at 200 rpm for 17 h, and the absorbance at 600 nm (OD₆₀₀) were measured to identify the lowest concentrations with no observable cell growth.

4.3. Protein Purification, Sodium Dodecyl Sulfate-Polyacrylamide Gel Electrophoresis (SDS-PAGE), and Western Blot Analysis. Five milliliters of cells were cultured overnight at 28 °C with shaking at 250 rpm. The next morning, cells were pelleted and resuspended in 1 mL of phosphate buffer containing 10 mM iodoacetamide (IAM) and phenylmethylsulphonyl fluoride (PMSF) (1:1000 dilution of a saturated ethanol solution), and sonicated for 1 min followed by centrifugation for 10 min at 15 000 rpm. The supernatant was removed, and cell pellets were resuspended in 0.2 mL of phosphate-buffered saline (PBS) + 2% Triton-X100 containing 10 mM IAM. The samples were incubated at room

Table 3. Engineered Disulfide Bonds in AcrB^a

Res1	Res2	oligomer (%)	activity level	citation
Inter-Sub	unit			
G51	A215	60.6 ± 6.80	+++	this study
Q123	P116	53.2 ± 11.4	++	
S167	N70	58.3 ± 5.4	+++	
F316	Q687	68.9 ± 6.4	_	
Q726	S233	69.1 ± 6.6	+++	
R765	G689	74.9 ± 6.8	_	
V105C	V105C	57.9 ± 13.2	+	
Q229	R586	46.4 ± 0.5	++	37
R558	E839	$-9.5 \pm 4.7e$	+++	
S562	T837	$15.4 \pm 1.3e$	+	
S132	A294	41.6 ± 0.6	+	
V32	A298	41.3 ± 1.2	+	
V32	A299	18.1 ± 1.0	+++	
Q726	S233	17.0 ± 0.4	+++	
I235	K728	23.8 ± 0.6	+++	
V225	A777	80.2 ± 1.3	+++	
Q229	T583	69.4 ± 0.5	+	
D566	T678	N/A	+	27, 32
F666	T678	N/A	_	
F666	Q830	N/A	+	
F316	Q687	N/A	++	27
F316	A688	N/A	+	
F316	G854	N/A	_	
Intra-Sub	unit			
V32	I390	82.5 ± 6.8	+++	39
T44	T91	100.7 ± 3.0	+++	
M184	V771	76.2 ± 4.9	+++	
T199	T749	82.7 ± 2.9	+++	
I335	A995	51.7 ± 0.8	+++	
T574	A627	102.9 ± 6.8	+++	
Q726	G812	97.7 ± 5.0	+++	
G570	A627		+++	
F572	A627		+++	
V576	A627		+++	
L578	A627		+++	

"+++: MIC equals to 50–100% of the wild-type MIC. ++: MIC equals to 25% of the wild-type MIC. +: MIC equals to 12.5% or less of the wild-type MIC. -: MIC close to the negative control MIC.

temperature with shaking for 45 min and centrifuged again for 10 min. The supernatant was used for SDS-PAGE and Western blot analysis.

For Western blot analysis, a disulfide bond was reduced either by incubating with 10% β -mercaptoethanol (BME) for 10 min or 50 mM dithiothreitol (DTT) for 1 h as indicated. After transferring to the poly(vinylidene difluoride) (PVDF) membrane, protein bands were detected using an anti-AcrB polyclonal (Rabbit) antibody raised to recognize a C-terminal peptide corresponding to residues number 1036–1045. The membrane was then washed and incubated with an alkaline phosphatase-conjugated Goat anti-Rabbit secondary antibody. The BCIP/NBT (5-bromo-4-chloro-3'-indolyphosphate and nitro-blue tetrazolium) solution was used to stain the membranes.

4.4. EtBr Accumulation Assay. The EtBr accumulation assay was performed following the established procedure with slight modification. Briefly, cells were grown in 15 mL of LB media until the mid-log phase (OD_{600} of 0.6-0.8). The bacteria were then centrifuged at 3000g for 15 min and washed

Table 4. Primers Used in the Study

construct	primer (5'-3')
AcrB_G51C_F	CCTCCTACCCCTGTGCTGATGCGAAAAC
AcrB_G51C_R	GTTTTCGCATCAGCACAGGGGTAGGAGG
AcrB_A215C_F	GAACGCCCAGGTTTGTGCGGGTCAGCTC
AcrB_A215C_R	GAGCTGACCCGCACAAACCTGGGCGTTC
AcrB_Q123C_F	CGCAAGAAGTTTGTCAGCAAGGGGTG
AcrB_Q123C_R	CACCCCTTGCTGACAAACTTCTTGCG
AcrB_P116C_F	CAGCTGGCGATGTGTTTGCTGCCGCAAGAAG
AcrB_P116C_R	CTTCTTGCGGCAGCAAACACATCGCCAGCTG
AcrB_S167C_F	GAAAGATGCCATCTGTCGTACGTCGGGC
AcrB_S167C_R	GCCCGACGTACGACAGATGGCATCTTTC
AcrB_N70C_F	GAACAGAATATGTGCGGTATCGATAACC
AcrB_N70C_R	GGTTATCGATACCGCACATATTCTGTTC
AcrB_F316C_F	GAAGATGGAACCGTGTTTCCCGTCGGG
AcrB_F316C_R	CCCGACGGAAACACGGTTCCATCTTC
AcrB_Q687C_F	GAGCTGATTGACTGTGCTGGCCTTGGTC
AcrB_Q687C_R	GACCAAGGCCAGCACAGTCAATCAGCTC
AcrB_Q726C_F	GAAGATACCCCGTGCTTTAAGATTGATATCG
AcrB_Q726C_R	CGATATCAATCTTAAAGCACGGGGTATCTTC
AcrB_S233C_F	CAGCTTAACGCCTGCATTATTGCTCAG
AcrB_S233C_R	CTGAGCAATAATGCAGGCGTTAAGCTG
AcrB_R765C_F	CGACTTTATCGACTGTGGTCGTGTGAAG
AcrB_R765C_R	CTTCACACGACCACAGTCGATAAAGTCG
AcrB_G689C_F	GATTGACCAGGCTTGCCTTGGTCAC
AcrB_G689C_R	GTGACCAAGGCAAGCCTGGTCAATC
AcrB Seq. 2_R	GTGTTGCACGCATGGTAATC
AcrB Seq. 3_R	CCATTGCTTCACCGGTACTT

once with 50 mM Na-Pi buffer, pH 7.4 under the same condition. The cells were then resuspended in the same buffer to adjust the OD_{600} of the cellular suspension as 2.0. 1 mL of the cell suspension was loaded into a cuvette and monitored using a fluorescence spectrometer (Perkin-Elmer LS 550), at excitation and emission wavelengths of 520 and 590 nm, respectively. After ~40 s, 1 mL of EtBr was added to a final concentration of 10 $\mu\mathrm{M}$ and to make final OD_{600} of cell suspension 1.0, and the emission was monitored for an additional 600 s. For the samples with DTT treatment, cells were incubated with 50 mM freshly prepared DTT for 1 h at room temperature before loading into the cuvette.

ASSOCIATED CONTENT

Accession Codes

AcrB, UniprotKB ID P31224

AUTHOR INFORMATION

Corresponding Author

Yinan Wei — Department of Chemistry, University of Kentucky, Lexington, Kentucky 40506, United States; orcid.org/0000-0002-9936-7149; Email: Yinan.wei@uky.edu

Authors

Prasangi Rajapaksha — Department of Chemistry, University of Kentucky, Lexington, Kentucky 40506, United States Ankit Pandeya — Department of Chemistry, University of Kentucky, Lexington, Kentucky 40506, United States

Complete contact information is available at: https://pubs.acs.org/10.1021/acsomega.0c02921

Notes

The authors declare no competing financial interest.

ACKNOWLEDGMENTS

The authors thank Dr. Attilio Vittorio Vargiu (Università degli studi di Cagliari, Cagliari, Sardinia, Italy) for critical reading and suggestions of this manuscript. This work is supported by NIH (Grant Numbers 1R56AI137020 and 1R21AI142063-01) and NSF (Grant Number CHE-1709381).

REFERENCES

- (1) Nikaido, H. Multiple antibiotic resistance and efflux. Curr. Opin. Microbiol. 1998, 1, 516–523.
- (2) Zgurskaya, H. I.; Nikaido, H. Multidrug resistance mechanisms: drug efflux across two membranes. *Mol. Microbiol.* **2000**, *37*, 219–225.
- (3) Sulavik, M. C.; Houseweart, C.; Cramer, C.; Jiwani, N.; Murgolo, N.; Greene, J.; DiDomenico, B.; Shaw, K. J.; Miller, G. H.; Hare, R.; et al. Antibiotic susceptibility profiles of *Escherichia coli* strains lacking multidrug efflux pump genes. *Antimicrob. Agents Chemother.* **2001**, *45*, 1126–1136.
- (4) Eswaran, J.; Koronakis, E.; Higgins, M. K.; Hughes, C.; Koronakis, V. Three's company: component structures bring a closer view of tripartite drug efflux pumps. *Curr. Opin. Struct. Biol.* **2004**, *14*, 741–747.
- (5) Nikaido, H. Multidrug efflux pumps of Gram-negative bacteria. *J. Bacteriol.* **1996**, *178*, 5853.
- (6) Du, D.; Wang, Z.; James, N. R.; Voss, J. E.; Klimont, E.; Ohene-Agyei, T.; Venter, H.; Chiu, W.; Luisi, B. F. Structure of the AcrAB—TolC multidrug efflux pump. *Nature* **2014**, *509*, 512–515.
- (7) Zwama, M.; Yamaguchi, A. Molecular mechanisms of AcrB-mediated multidrug export. *Res. Microbiol.* **2018**, *169*, 372–383.
- (8) Zwama, M.; Yamasaki, S.; Nakashima, R.; Sakurai, K.; Nishino, K.; Yamaguchi, A. Multiple entry pathways within the efflux transporter AcrB contribute to multidrug recognition. *Nat. Commun.* **2018**, *9*, No. 124.
- (9) Kim, J.-S.; Jeong, H.; Song, S.; Kim, H.-Y.; Lee, K.; Hyun, J.; Ha, N.-C. Structure of the tripartite multidrug efflux pump AcrAB-TolC suggests an alternative assembly mode. *Mol. Cell* **2015**, *38*, 180.
- (10) Daury, L.; Orange, F.; Taveau, J.-C.; Verchère, A.; Monlezun, L.; Gounou, C.; Marreddy, R. K.; Picard, M.; Broutin, I.; Pos, K. M.; et al. Tripartite assembly of RND multidrug efflux pumps. *Nat. Commun.* **2016**, *7*, No. 10731.
- (11) Wang, Z.; Fan, G.; Hryc, C. F.; Blaza, J. N.; Serysheva, I. I.; Schmid, M. F.; Chiu, W.; Luisi, B. F.; Du, D. An allosteric transport mechanism for the AcrAB-TolC multidrug efflux pump. *eLife* **2017**, *6*, No. e24905.
- (12) Shi, X.; Chen, M.; Yu, Z.; Bell, J. M.; Wang, H.; Forrester, I.; Villarreal, H.; Jakana, J.; Du, D.; Luisi, B. F.; et al. In situ structure and assembly of the multidrug efflux pump AcrAB-TolC. *Nat. Commun.* **2019**, *10*, No. 2635.
- (13) Murakami, S.; Nakashima, R.; Yamashita, E.; Yamaguchi, A. Crystal structure of bacterial multidrug efflux transporter AcrB. *Nature* **2002**, *419*, 587.
- (14) Pos, K. M.; Schiefner, A.; Seeger, M. A.; Diederichs, K. Crystallographic analysis of AcrB. FEBS Lett. 2004, 564, 333–339.
- (15) Murakami, S.; Nakashima, R.; Yamashita, E.; Matsumoto, T.; Yamaguchi, A. Crystal structures of a multidrug transporter reveal a functionally rotating mechanism. *Nature* **2006**, 443, 173–179.
- (16) Sennhauser, G.; Amstutz, P.; Briand, C.; Storchenegger, O.; Grütter, M. G. Drug export pathway of multidrug exporter AcrB revealed by DARPin inhibitors. *PLoS Biol.* **2006**, *5*, No. e7.
- (17) Das, D.; Xu, Q. S.; Lee, J. Y.; Ankoudinova, I.; Huang, C.; Lou, Y.; DeGiovanni, A.; Kim, R.; Kim, S.-H. Crystal structure of the multidrug efflux transporter AcrB at 3.1 Å resolution reveals the N-terminal region with conserved amino acids. *J. Struct. Biol.* **2007**, *158*, 494–502.
- (18) Törnroth-Horsefield, S.; Gourdon, P.; Horsefield, R.; Brive, L.; Yamamoto, N.; Mori, H.; Snijder, A.; Neutze, R. Crystal structure of AcrB in complex with a single transmembrane subunit reveals another twist. *Structure* **2007**, *15*, 1663–1673.

- (19) Murakami, S. Multidrug efflux transporter, AcrB—the pumping mechanism. *Curr. Opin. Struct. Biol.* **2008**, *18*, 459–465.
- (20) Nakashima, R.; Sakurai, K.; Yamasaki, S.; Nishino, K.; Yamaguchi, A. Structures of the multidrug exporter AcrB reveal a proximal multisite drug-binding pocket. *Nature* **2011**, *480*, 565–569.
- (21) Kobylka, J.; Kuth, M. S.; Müller, R. T.; Geertsma, E. R.; Pos, K. M. AcrB: a mean, keen, drug efflux machine. *Ann. N. Y. Acad. Sci.* **2020**, *1459*, 38–68.
- (22) Eicher, T.; Seeger, M. A.; Anselmi, C.; Zhou, W.; Brandstätter, L.; Verrey, F.; Diederichs, K.; Faraldo-Gómez, J. D.; Pos, K. M. Coupling of remote alternating-access transport mechanisms for protons and substrates in the multidrug efflux pump AcrB. *eLife* **2014**, 3. No. e03145.
- (23) Zhang, X. C.; Liu, M.; Han, L. Energy coupling mechanisms of AcrB-like RND transporters. *Biophys. Rep.* **2017**, *3*, 73–84.
- (24) Li, X.-Z.; Plésiat, P.; Nikaido, H. The challenge of efflux-mediated antibiotic resistance in Gram-negative bacteria. *Clin. Microbiol. Rev.* **2015**, 28, 337–418.
- (25) Oswald, C.; Tam, H.-K.; Pos, K. M. Transport of lipophilic carboxylates is mediated by transmembrane helix 2 in multidrug transporter AcrB. *Nat. Commun.* **2016**, *7*, No. 13819.
- (26) Seeger, M. A.; Schiefner, A.; Eicher, T.; Verrey, F.; Diederichs, K.; Pos, K. M. Structural asymmetry of AcrB trimer suggests a peristaltic pump mechanism. *Science* **2006**, *313*, 1295–1298.
- (27) Takatsuka, Y.; Nikaido, H. Site-directed disulfide cross-linking shows that cleft flexibility in the periplasmic domain is needed for the multidrug efflux pump AcrB of *Escherichia coli. J. Bacteriol.* **2007**, *189*, 8677–8684.
- (28) Seeger, M. A.; Diederichs, K.; Eicher, T.; Brandstatter, L.; Schiefner, A.; Verrey, F.; Pos, K. M. The AcrB efflux pump: conformational cycling and peristalsis lead to multidrug resistance. *Curr. Drug Targets* **2008**, *9*, 729–749.
- (29) Takatsuka, Y.; Nikaido, H. Covalently linked trimer of the AcrB multidrug efflux pump provides support for the functional rotating mechanism. *J. Bacteriol.* **2009**, *191*, 1729–1737.
- (30) Schulz, R.; Vargiu, A. V.; Collu, F.; Kleinekathöfer, U.; Ruggerone, P. Functional rotation of the transporter AcrB: insights into drug extrusion from simulations. *PLoS Comput. Biol.* **2010**, *6*, No. e1000806.
- (31) Vargiu, A. V.; Ramaswamy, V. K.; Malvacio, I.; Malloci, G.; Kleinekathöfer, U.; Ruggerone, P. Water-mediated interactions enable smooth substrate transport in a bacterial efflux pump. *Biochim. Biophys. Acta, Gen. Subj.* 2018, 1862, 836–845.
- (32) Takatsuka, Y.; Nikaido, H. Site-directed disulfide cross-linking to probe conformational changes of a transporter during its functional cycle: *Escherichia coli* AcrB multidrug exporter as an example. *Methods Mol. Biol.* **2010**, 634, 343–354.
- (33) Craig, D. B.; Dombkowski, A. A. Disulfide by Design 2.0: a web-based tool for disulfide engineering in proteins. *BMC Bioinf.* **2013**, *14*, No. 346.
- (34) Murakami, S.; Tamura, N.; Saito, A.; Hirata, T.; Yamaguchi, A. Extramembrane central pore of multidrug exporter AcrB in *Escherichia coli* plays an important role in drug transport. *J. Biol. Chem.* **2004**, *279*, 3743–3748.
- (35) Yu, L.; Lu, W.; Wei, Y. AcrB trimer stability and efflux activity, insight from mutagenesis studies. *PLoS One* **2011**, *6*, No. e28390.
- (36) Schindelin, J.; Arganda-Carreras, I.; Frise, E.; Kaynig, V.; Longair, M.; Pietzsch, T.; Preibisch, S.; Rueden, C.; Saalfeld, S.; Schmid, B.; Tinevez, J.-Y.; White, D. J.; Hartenstein, V.; Eliceiri, K.; Tomancak, P.; Cardona, A. Fiji: an open-source platform for biological-image analysis. *Nat. Methods* **2012**, *9*, 676–682.
- (37) Seeger, M. A.; Von Ballmoos, C.; Eicher, T.; Brandstätter, L.; Verrey, F.; Diederichs, K.; Pos, K. M. Engineered disulfide bonds support the functional rotation mechanism of multidrug efflux pump AcrB. *Nat. Struct. Mol. Biol.* **2008**, *15*, 199.
- (38) Parmar, M.; Rawson, S.; Scarff, C. A.; Goldman, A.; Dafforn, T. R.; Muench, S. P.; Postis, V. L. Using a SMALP platform to determine a sub-nm single particle cryo-EM membrane protein structure. *Biochim. Biophys. Acta, Biomembr.* **2018**, *1860*, 378–383.

- (39) Lu, W.; Zhong, M.; Wei, Y. A reporter platform for the monitoring of in vivo conformational changes in AcrB. *Protein Pept. Lett.* **2011**, *18*, 863–871.
- (40) Lu, W.; Zhong, M.; Chai, Q.; Wang, Z.; Yu, L.; Wei, Y. Functional relevance of AcrB trimerization in pump assembly and substrate binding. *PLoS One* **2014**, *9*, No. e89143.
- (41) Wang, Z.; Ye, C.; Zhang, X.; Wei, Y. Cysteine residue is not essential for CPM protein thermal-stability assay. *Anal. Bioanal. Chem.* **2015**, 407, 3683–3691.
- (42) Humphries, R. M.; Ambler, J.; Mitchell, S. L.; Castanheira, M.; Dingle, T.; Hindler, J. A.; Koeth, L.; Sei, K. CLSI Methods Development and Standardization Working Group of the Subcommittee on Antimicrobial Susceptibility Testing. CLSI Methods Development and Standardization Working Group Best Practices for Evaluation of Antimicrobial Susceptibility Tests. J. Clin. Microbiol. 2018, 56, No. e01934-17.
- (43) Paixão, L.; Rodrigues, L.; Couto, I.; Martins, M.; Fernandes, P.; De Carvalho, C. C.; Monteiro, G. A.; Sansonetty, F.; Amaral, L.; Viveiros, M. Fluorometric determination of ethidium bromide efflux kinetics in *Escherichia coli*. *J. Biol. Eng.* **2009**, *3*, No. 18.